

Mono Tiltrotor (MTR) Validation Activities

G. Douglas Baldwin*
Baldwin Technology Company, LLC
Port Washington
New York 11050

Abstract

The Mono Tiltrotor (MTR) is a proposed, innovative cargo rotorcraft architecture. The capabilities of the MTR are predicated on the combination of an advanced coaxial rotor system and sophisticated kinematics that morph the aircraft topology for efficient flight over the entire operational envelope. The MTR rotorcraft integrates a coaxial rotor, a folding lifting wing system, a lightweight airframe and an efficient cargo handling system that is capable of rapidly and economically transporting a variety of mission tailored payloads. This paper summarizes MTR validation activities performed from June 2007 through March 2008, including flight hardware demonstrations and independent engineering assessments.

Introduction

An Army Aviation Applied Technology Directorate (AATD) contract was let to Baldwin Technology Company, LLC (BTC) to advance the understanding of the Mono Tiltrotor (MTR) aircraft architecture [1]. A first task order to design a 9,400 pound gross weight MTR Scaled Demonstrator (MTR-SD) and perform subscale wind tunnel tests of key features was completed in 2006 [2] and summarized in an AHS International Specialists Meeting 2007 paper [3]. A second task order is underway to build and flight test key features of the MTR, integrate these features into an MTR Functional Demonstrator (MTR-FD), and also hire 3rd party engineering authorities to perform independent assessments of the MTR-SD.

Subject

The Mono Tiltrotor (MTR) is a proposed, innovative cargo rotorcraft architecture [4, 5]. The capabilities of the MTR are predicated on the combination of an advanced coaxial rotor system and sophisticated kinematics that morph the aircraft topology for efficient flight over the entire operational envelope. The MTR rotorcraft integrates a coaxial proprotor, a folding lifting wing system, a lightweight airframe and an efficient cargo handling system that is capable of rapidly and economically transporting a variety of mission tailored payloads.

Purpose

Under the current Army AATD task order, BTC is leading the development and testing of functional flight demonstration hardware and has hired reputable 3rd party firms to perform independent engineering assessments of the MTR Scaled Demonstrator (MTR-SD). Flight hardware build and test was performed at the Georgia Institute of Technology, while an independent design assessment was performed by Bell Helicopter Textron Incorporated (BHTI), and an independent Computational Fluid Dynamics (CFD) drag assessment was performed by the proprietor of Scientific Simulations Inc., Dr. Dimitri Mavriplis.

Scope

The scope of this paper is to report on work performed to-date under the current AATD task order. Completed work includes flight demonstrations of key MTR features, an independent design assessment, and a CFD drag assessment of the MTR-SD. Flight testing of the integrated MTR-FD is in progress.

Plan

The work plan included the following two parallel activities:

Hardware Flight Test

The key innovative features of the MTR air vehicle architecture were itemized in an AHS Forum 2007 paper [6], namely: 1) aerodynamically deployed wing panels,

* Managing Director. doug@baldwintech.com

Presented at 64th Annual Forum and Technology Display of the American Helicopter Society International, Montreal, Canada, April 29 – May 1, 2008. Copyright © 2008 by the American Helicopter Society International, Inc. All rights reserved.

2) pitch axis suspended load, and 3) tilting coaxial proprotor. A plan for fundamental prototyping and flight demonstration of these features, both in isolation and as an integrated system, was decided. Remote Control (RC) aircraft rapid prototyping techniques were used to build each feature. Flight testing always began with known working aircraft configurations, and incremental modifications were added until the target demonstration was achieved. While each feature was being independently flight tested, a new MTR Functional Demonstrator (MTR-FD) was designed to integrate these features. Furthermore, the plan includes capturing MTR-FD telemetry, replicating aircraft flight dynamics in a ground based simulator, applying the simulator data to developing and then flight testing autonomous control laws, and subsequently scaling up the observed dynamic behavior to the MTR-SD design.

Independent Engineering Assessments

A plan for generating an authoritative assessment of the MTR-SD was decided. BTC delivered to BHTI a copy of the first task order final report [2], which includes MTR-SD design data, and subsequently contracted with BHTI to provide a limited, independent assessment of the MTR-SD [7] design based exclusively on this report. Differences identified between the MTR-SD final report numbers and BHTI's initial predictions, primarily in the area of the prediction of boundary layer separation drag due to aft body contraction of the original configuration, lead to a geometric streamlining and computational fluid dynamics (CFD) analysis by BTC showing aft body contraction would not cause separation drag. An extension of the original contract was provided by BTC for BHTI to complete the evaluation of the original configuration assuming no aft body separation drag. To supplement this assessment, BTC subsequently contracted with Scientific Simulations Inc. to accurately predict the equivalent flat plate drag of the streamlined geometry using validated CFD codes [8]. The results of the CFD drag assessment were then factored into the BHTI performance results.

Research Methodology

The research methodology included two parallel activities: hardware flight tests and independent engineering assessments.

Hardware Flight Tests

The following description of hardware flight tests is best illustrated in video format. For that reason, photos are omitted and the reader is encouraged to view a publicly released video of hardware flight tests conducted during

the summer of 2007 [9]. This video was first presented at the Association for Unmanned Vehicle Systems International (AUVSI) Lone Star Chapter Meeting on 06 Nov 2007.

As a first step towards achieving RC scale hardware flight tests, the MTR-SD 9,400 pound gross weight design needed to be scaled down to an RC sized vehicle. Since the most complex subsystem would be the coaxial drive, a survey of commercially available coaxial hardware was undertaken. It was decided to use the Cad u. Modelltechnik Jung CRM-T coaxial mechanics [10] with 2.0 meter diameter blades driven by an 8 horsepower JetCat SPT-5H kerosene fueled turboshaft engine [11]. With this decided, work could begin towards designing an MTR-FD (Figure 1).

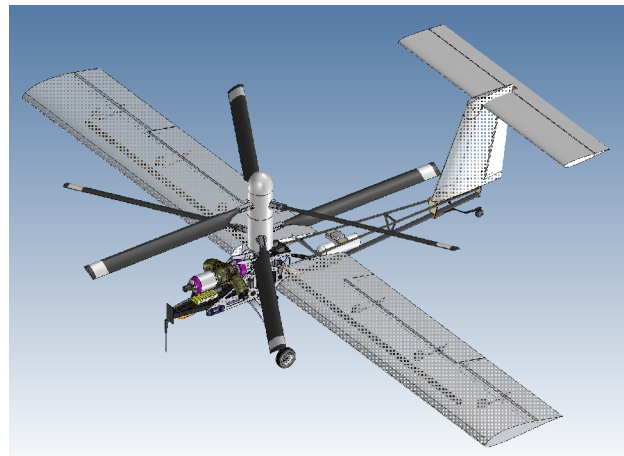


Figure 1: Rendering of MTR Functional Demonstrator (MTR-FD) design.

With the MTR-FD design project underway, a separate work project was initiated to build and test aerodynamically deployed wings, pitch axis suspended load, and tilting rotor using a Century Raven 50 [12] helicopter test platform, modified with a 3-bladed fly-bar-less rotor head [13]. The multi-blade head was selected to be most similar to the MTR-FD design which has 3 blades per hub. A key advantage of this Century helicopter for MTR demonstrations is its unobstructed lateral opening at the helicopter's center of gravity (CG), providing room for adding a pitch axis bearing block for the suspended load, a wing spar at the aircraft CG, and a suitable location for having a rotor tilt axis.

Aerodynamically Actuated Wings

Detailed design of the aerodynamically deployed wing panel subsystem evolved during a series of flight experiments and hardware modifications. After completing pilot familiarization with the multi-bladed Century 50, a 3/4 inch thick polystyrene foam-board center wing panel was mounted onto the tailboom and flight

tested. Next, short lateral polystyrene foam-board wing panels were attached by taped hinges to this center wing panel and flight tested. The short wing panels were then replaced by increasingly larger lateral wing panels until the fully deployed wing span was approximately double the rotor diameter.

A landing procedure with the hinged wings was developed during a series of flight tests. An initial landing technique was developed where the pilot hovered the aircraft with the wingtips suspended immediately above the runway. Then, in a single motion of forward and downward movement of the helicopter, the wing panels flared out as the wingtips touched down and the helicopter landed. The flaring motion of the wing panels was speculatively attributed to rotor downwash deflection by the runway, supplemented by airfoil generated lift as the vehicle moved slightly forward. While this technique was satisfactory for the lightweight foam-board wing panels, it was expected to be unacceptable for heavier, load bearing wings panels. Wingtip mounted wheels were added and fixed at an angle designed to drive the wingtips outward as the vehicle moved forward. With this hardware modification, an improved landing technique was developed where the pilot descended until the wingtip mounted wheels touched the ground, and then moved the aircraft forward slightly to drive the wingtips outward while the helicopter landed.

With the fundamental wing panel design decided and the landing technique developed, the next step was to design, build, and test load bearing wing panels incorporating a remotely controlled hinge locking and unlocking mechanism. The load bearing wing design included a tubular spar passing through the helicopter CG. The spar tube was cut at the wing hinge, and a technique for connecting these discontinuous spar tubes at the instant of full wing deployment was devised. The technique included an electrical contact switch to sense full wing panel deployment, and a pair of plungers at the center wing panel which were pneumatically driven into the outer wing panel spar tubes. The pilot's remote controller included a switch to either arm the locks or to retract the locks. A piloting procedure was developed where the aircraft was flown in slow straight or turning flight with the wing panels partially deployed, and when ready to achieve deployment the pilot arms the locks and increases the helicopter's angle of attack to lift the wing panels into position. The piloting procedure for wing panel recovery was to maintain wing loading while retracting the spar plunger. As the flight speed was then decreased, the wing panels would slowly descend. This wing deployment and recovery technique proved to be repeatable and controllable. The landing procedure with the load bear wing panels was identical to landing with the lightweight foam board wing panels, using wingtip mounted wheels to drive the wing panels outward as the

helicopter moved forward while landing. Landing was accomplished in upwind, sidewind, and downwind conditions. It was observed that in hover the heavier load bearing wing panels hung straight down with their span aligned with the rotor wake.

Pitch Axis Suspended Load

Detailed design of the pitch axis suspended load evolved during a series of flight experiments and hardware modifications. Lateral bearing blocks were mounted onto the Century 50 at its CG, and a freely rotating shaft was inserted into the bearing blocks. Rigid suspension struts were mounted to either end of the rotating shaft. Small wheels were mounted to the lower ends of the suspension struts to facilitate development of a landing procedure. The RC pilot found that when the suspension strut wheels touched the runway, the struts would tend to roll either forward or aft as the helicopter landed.

Next, a lead weight was tied by cables to the lower end of the suspension struts. A landing procedure for this configuration was developed in which the lead weight was lowered onto the runway, and then the helicopter moved forward while landing. The cables allowed the lead weight to touch down without the suspension struts hitting the ground. After the pilot became comfortable with this configuration, progressively heavier lead weight was added. Eventually, the total weight of suspended load comprised 40% of the vehicle gross weight. The pilot found that pitch stability and control was unaffected by the magnitude of the weight, which was attributed to the fact that the suspension struts were pivotally attached at the helicopter pitch axis.

The lead weight was then replaced by a prototypical cargo pod (aka suspended fuselage), incorporating a vertical and horizontal stabilizer, rudder, and elevator. This configuration was flown both with fixed elevator and rudder positions, and with actively controlled elevator and rudder. Both control methods were found to be feasible. Active controls allowed for the cargo pod to achieve longitudinal trim in forward flight and to have a coordinated turn with the helicopter.

Tilting Centerline Rotor

The folding wing system described above was modified into a fixed wing platform for conducting tilting centerline rotor tests. An airplane tailboom with empennage was added to the wing, and a conversion actuator rotated the helicopter relative to this fixed wing platform. Heading hold gyros were added to the helicopter about its pitch, roll, and yaw axes, and the rotor roll and yaw controls were mixed in coordination with rotor tilt angle. Helicopter mode take off was achieved with this platform, and in forward flight the

rotor was tilted to its mechanical limit of 25 degrees from airplane mode. Conversion was stable and controllable, and piloting procedures were developed that can be applied to the MTR-FD platform.

MTR-FD

The MTR-FD was designed in the fall of 2007, fabricated over the winter, and instrumented in the first quarter of 2008. In March 2008, the aircraft achieved first hovering flight with fixed wings attached.

Independent Engineering Assessments

Authoritative 3rd party engineering assessments of the MTR-SD were performed in the areas of weight, drag, hover efficiency, propulsive efficiency, flight dynamics, and airplane mode cruise performance. The following sections are largely verbatim from the subcontractor reports, with edits for brevity and clarification. The source material for these assessments was exclusively the task order one final report [2], unless otherwise noted.

Weight

BHTI re-organized the MTR-SD final report weights along the lines of the industry accepted MIL-STD-1374 Part I weight statement, then performed a 'bottoms-up' weight estimate that produces an overall aircraft weight empty. Table 1 summarizes the weight evaluation and also assigns a 'weight risk level' assessment to each category. BHTI determined that those areas labeled 'high' risk are in danger of not attaining the MTR-SD reported weight goal either because it is underestimated or is not sufficiently developed to be confident in the estimated weight. Those areas labeled 'medium' risk pose a moderate danger of not attaining the weight goal. The current weight allocation may be sufficient but if the development of the structure and the integration of the systems into the air vehicle are not properly addressed, the weight penalties could be substantial. The 'low' risk areas are considered to have sufficient weight allocation. However, all the weight assessments are based on certain assumptions. Listed below is a description of the areas evaluated, what components are considered to be part of that area, and the design assumptions that were central to the weight assessments.

Wing Group: This group includes all primary and secondary wing structure, including the flaps and the fold mechanism. The flap control actuators are not included in this group but are accounted for in the Flight Controls Group. The weight estimate assumes that composite structure will be extensively used and that the most current design practices will be employed to produce a light weight design.

Rotor Group: This group includes the main rotor blades and hubs and the spinner. It does not include the main rotor masts or any of the main rotor controls which are accounted for in the Drive System Group and the Flight Controls Group respectively. The BHTI weight estimate assumes that there is neither fold capability nor any provisions for anti-icing or vibration dampening (pendulums). It has also been assumed that the spinner will be designed to sustain required bird strike criteria.

Tail Group: This group includes a single vertical tail and a single horizontal stabilizer. It does not include the tail boom structure. The weight calculation assumes the MTR-SD design report method of construction for both the horizontal and vertical tails (constant section aluminum I-beam the entire span of the structure), but this is not considered to be weight efficient and provides an opportunity for significant weight reduction.

Body Group: This group includes the tail boom structure and all other structural elements required to provide adequate load paths to adjoin the tail boom, pylon/rotors, engine section, fuel system, and avionic/instrument compartments. The intent is to suspend all structural components from a single central location, including the main gearbox with the engines attached to it. The aircraft structure needs to be further developed in order to accurately assess the weight impact.

Landing Gear Group: This group includes the landing struts attached to the pylon assembly and a contact point at the extreme end of the tail boom. The weight estimation assumes that the alighting gear is designed to at least a 12 fps descent rate at design gross weight and has no wheels or tires.

Nacelle Group: This group includes the engine mounts, engine firewalls, and the nacelle or cowling structure that surrounds the engines and its systems. The BHTI weight estimation assumes that extensive use of composite structure will be used. The intent of the MTR-SD report may have been to account for these items in other areas such as the Body Group or Engine Installation, but sufficient weight has not been allocated in those areas to account for this structure. No mention of firewalls is made in the MTR-SD final report and the nacelle structure surrounding the engines, depicted in the illustrations, is not specified in the weight summaries. These items constitute significant weight in a typical aircraft.

Propulsion Group: This group consists of the engines, the engine start, controls, exhaust, and lubrication systems, and the fuel system. The weight estimation considers that the engine control system will be an electronic system employing a single FADEC per engine. The engine start system will use auxiliary power unit (APU) powered pneumatic starters. The lubrication

Table 1 - BHTI WEIGHT ASSESSMENT OF THE BALDWIN MONO TILTROTOR

<u>Design Group</u>	<u>MTR Nomenclature</u>	<u>MTR Weights (lb)</u>		<u>BHTI Weights (lb)</u>		<u>Delta</u>	<u>Weight Risk Level</u>
		<u>Two Engines</u>		<u>Two Engines</u>		<u>Weight (lb)</u>	
Wing Group		539		512		-27	LOW
	Wing (Center panel)		163				
	Wing (Side panels)		376				
	Wing Gearing/Tilt Mechanism		0				
Rotor Group		754		705		-49	LOW
	Upper Rotor (With Hub)		377				
	Lower Rotor (With Hub)		377				
Tail Group		229		165		-64	LOW
	Vertical Stabilizer		128				
	Horizontal Stabilizer		101				
Body Group		180		201		21	MEDIUM
	Hardpoints (2)		100				
	Tail Boom		26				
	Tilt Boom		54				
Landing Gear Group		104		107		3	LOW
	Landing Gear (Rotor Section)		104				
Nacelle Group				113		113	HIGH
Propulsion Group		891		848		-43	LOW
	Engine Weight (2/1)		680				
	Engine Installation Weight		74				
	Fuel System		137				
Drive System Group		1075		1046		-29	LOW
	Upper Rotor Shaft		75				
	Lower Rotor Shaft		65				
	Main Gear Box		685				
	Transmission Cross Shafts (2/1)		250				
Flight Controls Group		179		375		196	HIGH
	Upper Swashplate		62				
	Lower Swashplate		57				
	Automatic Flight Control System		incl in Avionics				
	Tilting Mechanism (Actuator)		60				
APU Group		101		118		17	MEDIUM
	Auxiliary Power Unit		101				
Instruments/Avionics Groups		100		130		30	MEDIUM
	Instrumentation/Avionics/Furnishings		100				
Hydraulics Group		71		85		14	MEDIUM
	Control Hydraulics		71				
Electrical Group		90		119		29	MEDIUM
	Electrical System		90				
Load & Handling Group		49		52		3	LOW
	Trapeze (Payload) Struts (2)		49				
Weighted Configuration		----- 4362		----- 4577		----- 215	LOW / MEDIUM
Items Not Considered In This Weight Assessment		538		538			
	Cargo Handling System		200		200		
	Payload Longitudinal Stabilization		170		170		
	Payload Vertical Tail (2)		64		64		
	Payload Landing Gear		104		104		
MTR Weight Empty		----- 4900		----- 5115		----- 215	LOW / MEDIUM
Fuel - Full		1500		1500			
Payload (Available)		3000		2785			
MTR Gross Weight		----- 9400		----- 9400			

Table 1: BHTI weight assessment of the MTR-SD.

system is integral to the engine and consists only of usable oil (25 pounds). The fuel system consists of a single crashworthy fuel cell that contains 225 gallon of fuel.

Drive System Group: This group includes the main gearbox, the main rotor masts, the engine input drive trains (transmission cross shafts), and the main gearbox standpipe. The BHTI weight estimates for this group are based on established ‘best practices’ which are intended to produce safe, reliable drive systems.

Flight Controls Group: This group consists of the main rotors rotating controls, main rotor actuators, horizontal tail actuation, wing surface controls, and the pylon/tail boom conversion actuation. The weight estimation was based on the assumption that all flight control actuation is hydraulically powered by a 3000 psi hydraulic system. The rotating controls and six main rotor actuators will constitute more than half the weight required in this group.

APU Group: This group includes the auxiliary power unit (APU) and its installation. The weight estimation assumes an APU of 40 horsepower that will use bleed air for pneumatic engine starting. It also assumes that the APU will be electrically started using a battery accounted for in the Electrical Group below. Additional information about the APU or its installation is needed to lower its risk level.

Instrument/Avionics Group: This group consists of the instrument sensors and avionics equipment that are typically required on an unmanned air vehicle. The BHTI weight estimate is based on past experience in equipping a vehicle of this type (UAV) with the necessary communication and guidance equipment and properly protecting it from internal and external interferences (electromagnetic environmental effects {E3} shielding).

Hydraulics Group: This group includes the hydraulic system required to power the flight controls and pylon conversion systems. The weight estimation assumes that a 3000 psi system will be used and that it will provide hydraulics to approximately ten actuators throughout the aircraft.

Electrical Group: This area includes the electrical power generation components as well as the power distribution system. This weight estimate assumes a

13 amp-hour battery, one 12 kilovolt-amperes (kVA) generator, one 0.45 kVA inverter, and the wiring, relays, and circuit breakers required for normal electrical distribution to all electrical components in the aircraft.

Load & Handling Group: This group includes the cargo suspension ‘trapeze’ as well as aircraft tie down fittings. The MTR-SD final report analysis and weight derivation is considered an appropriate weight goal for this component. A few pounds were also added to this group to account for aircraft ground handling and tie down fittings.

Cargo Handling System: This group includes the cargo pod (aka fuselage) on the lower end of the ‘trapeze’. This structure was excluded as part of this analysis and was not evaluated. For purposes of comparison, the weight of this structure is represented as the final weight (538 pounds) in the MTR-SD final report.

First Order Drag Assessment

BHTI conducted a first order parasite drag evaluation based on the configuration in the MTR-SD final report [2], with further analysis by BTC showing that aft body contraction boundary layer separation drag could be avoided. The method of evaluation utilized a component build-up approach initially developed within the fixed-wing industry and carried over to the rotary-wing industry. The method is a combination of classic lifting surface and body of revolution analysis combined with empirical corrections for bluff body aerodynamics and manufacturing/operational variations. Individual component characteristic lengths, diameters, etc., and the design operation condition are defined (in this case the

Helo Mode				
Item	Baldwin	BHTI	Δf_e	
Spinner	2.254	4.200	1.946	
Exp Hub & grips	0	3.120	3.120	
Tailboom	0.246	0.459	0.213	
Nacelle/Fuel Tank	12.797	7.748	-5.049	(engine area extracted)
Wing Panels	1.223	1.670	0.447	
Alighting Gear	0.038	0.44	0.402	(deployed in helo mode)
V & H Tail	0.540	0.263	-0.277	
Struts	0.617	0.364	-0.253	
Fuselage fairings	0.014	0.0	-0.014	(included in fuselage)
Fuselage	1.013	1.287	0.274	(frontal only)
Fuse V-Tails	0.181	0.239	0.057	
Interference	3.785	0.0	-3.785	(included in each component)
sub totals	22.709	19.791	-2.919	
Protuberances	0	0.836	0.836	(% component total)
Trim	0	0.500	0.500	(estimated)
Momentum	0	0.383	0.383	(xsmn cooling, eng, etc.)
fe HELO MODE =	22.71	21.51	-1.20	

Table 2: BHTI drag assessment of the MTR-SD in helicopter mode. Quantities represent square feet of equivalent flat plate area.

200 knot [kt] cruise condition at 20,000 foot altitude [20k] International Standard Atmosphere [ISA]) from which operating Reynolds numbers and skin frictions are extracted. The drag contributions of the individual components are then determined from the net wetted areas, the skin friction values, and the empirical shape factors. Lifting surface contributions are evaluated on a net wetted area, defined plan form area, and drag coefficient. Bodies of revolution utilize a combination of “super velocity” evaluations of the component for streamlined bodies and bluff bodies. This includes fineness ratio, maximum perimeter, etc. The values are generally averaged and corrections for body shape factors (aft body ramp angles, etc.) are incorporated. Some values are modified based on proprietary

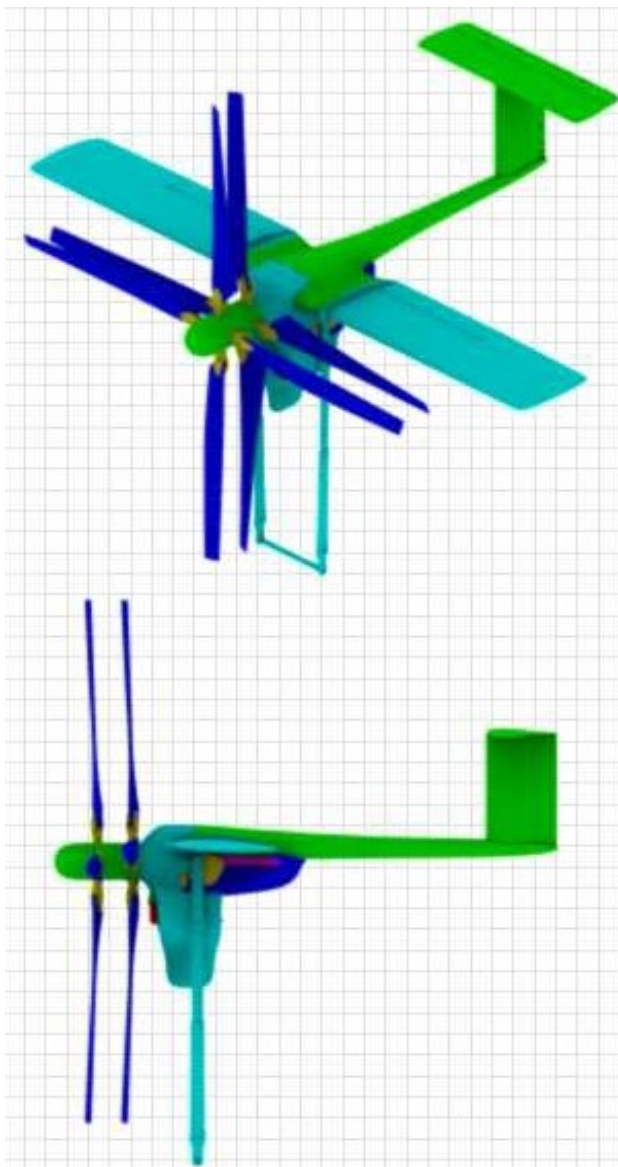


Figure 2: MTR configuration as illustrated in the MTR-SD final report.

configuration drag database results. Interference, gaps, seals, control surfaces, cooling and momentum variations are included. The contributions of the individual components are summarized in Table 2 for the helicopter mode of flight. The assessed risk levels to achieve the values of the MTR-SD final report are included in the summations and are highlighted in green, yellow, or red for low, medium, or high risk. The BHTI summary for the airplane mode of flight will be presented following the next section discussing CFD drag assessment.

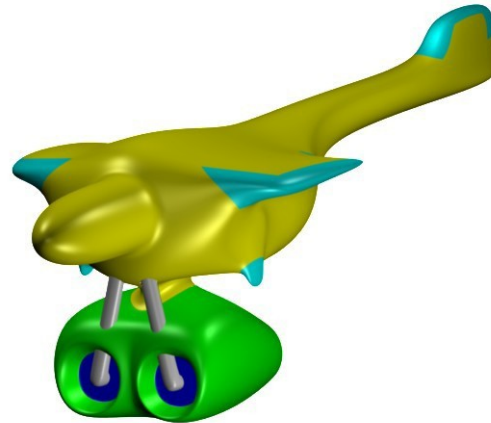


Figure 3: MTR-SD fuselage outer mold line with streamlined fuel tank and pod mounted turboshaft engines.

CFD Drag Assessment

In the process of demonstrating to BHTI that aft body separation could be avoided, BTC developed a fuselage outer mold line with streamlined fuel tank, and a streamlined cargo pod (aka fuselage). The BHTI first order drag assessment of the fuselage and fuel tank was based on the MTR-SD final report configuration shown at Figure 2, whereas the streamlined configuration with pod mounted turboshaft engines is shown at Figure 3. The teal colored surfaces shown in Figure 3 connect to uniform cross-section linear structures (wing, tail, and struts) that can be accurately predicted using the 1st order techniques described above. A similar streamlining was performed on the cargo pod. As a follow-on drag assessment activity, BTC hired Scientific Simulations LLC to perform a CFD drag assessment of these streamlined bodies. The objective of this study was to determine the drag on the subject geometries using the NSU3D unstructured mesh solver developed by Scientific Simulations which has been well validated for aerodynamic configurations. NSU3D has been a regular participant in the AIAA Drag prediction workshop series, where numerous industry and government aerodynamic CFD codes are compared for drag prediction accuracy and reliability on typical aircraft configurations [14, 15].

In order to compute the aerodynamic forces over the subject geometries, a suitable mesh with adequate resolution in critical areas of the flow field was generated. The steady-state flow-field was computed on this mesh using the NSU3D compressible Navier-Stokes solver. The results of the calculation were post-processed using the commercially available TECPLOT software.

For the fuselage with streamlined fuel tank, a half-geometry with a vertical plane of symmetry was used, since no sideslip conditions were considered. The total length of the airframe was 7.16 meters and the reference area used for the drag coefficient was 0.845308 square meters. The generated grid contained over 1.7M hexahedral cells with a first cell height of from 2.4e-6 meters to 7.9e-6 meters and cell height growth factor of 1.2 out to a distance of 20x the reference length. The surface resolution of this mesh was carefully tailored to obtain enhanced resolution in critical areas of the geometry and flow field, as shown in Figure 4.

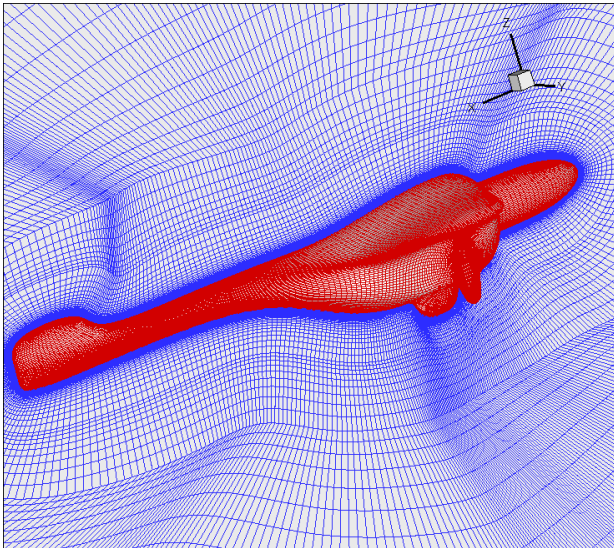


Figure 4: Illustration of hexahedral grid about MTR-SD fuselage with streamlined fuel tank. Total number of cells = 1.7 million.

A grid generation approach similar to that used for the fuselage was used for the cargo pod geometry. A quarter geometry with vertical and horizontal planes of symmetry was used, resulting in a grid with approximately 315,000 hexahedral cells, using a first cell height at the wall of from 4.1e-6 to 7.1e-6 meters, and extending out to 20x the reference length (3.508 meters). For brevity, an illustration of the mesh used for the cargo pod geometry is not shown.

NSU3D solves the compressible Reynolds-averaged Navier-Stokes (RANS) equations on unstructured meshes using arbitrary element types. NSU3D is a vertex-based scheme which operates on the dual-median control

volumes of the given mesh. The discretization uses matrix-based artificial dissipation, which has been found to be less dissipative than upwind schemes, and exhibits second-order accuracy in space. The Spalart-Allmaras turbulence model is used to simulate turbulence effects.

Because NSU3D operates in non-dimensional quantities, an input Mach number and Reynolds number were required for the simulation. Based on the nominal flight conditions and geometry dimensions (20k, 200 kts, 7.16 meters, 0 degrees incidence), the Mach number was computed to be 0.325 and the Reynolds number per meter was set to 4,224,901. The flow solver was run for 5000 iterations, using 2 grid levels in the multigrid sequence.

Figure 5 depicts the computed surface pressure coefficient values, while Figure 6 illustrates the Mach contour values on the symmetry plane (Mach being equal to zero on the no slip surfaces of the airframe). The figures indicate that the flow is attached over almost the entire geometry, an observation which has been verified by looking at velocity vector plots for this solution. Validation of the normal resolution used at the wall for this mesh is given in Figure 7, where the y^+ values plotted on the surface are seen to be less than 1 over virtually the entire airframe surface. The drag coefficient numbers provided in Table 3 are broken down into pressure and friction drag, defined using a reference area of 0.845308 square meters.

The degree of resolution used on the mesh conforms to the best practices typically used for aerodynamic calculations with NSU3D, and the drag values computed on this mesh can be considered to be reliable and accurate.

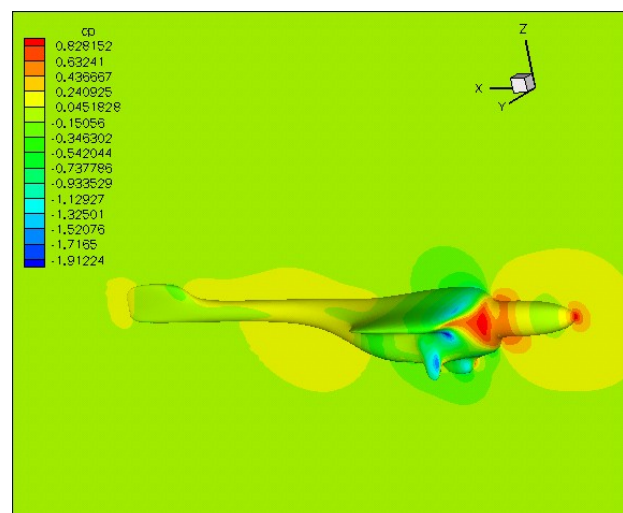


Figure 5: Computed pressure coefficient contours over MTR-SD fuselage with streamlined fuel tank at nominal conditions (Mach=0.325, Re=4.2M/m)

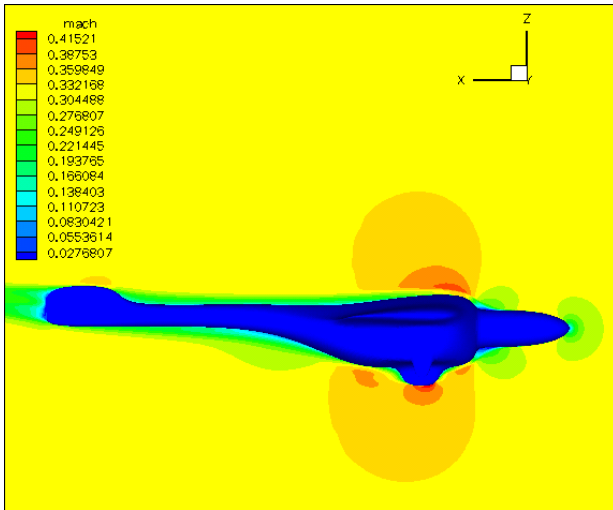


Figure 6: Computed Mach contours at symmetry plane over MTR-SD fuselage with streamlined fuel tank at nominal conditions (Mach=0.325,

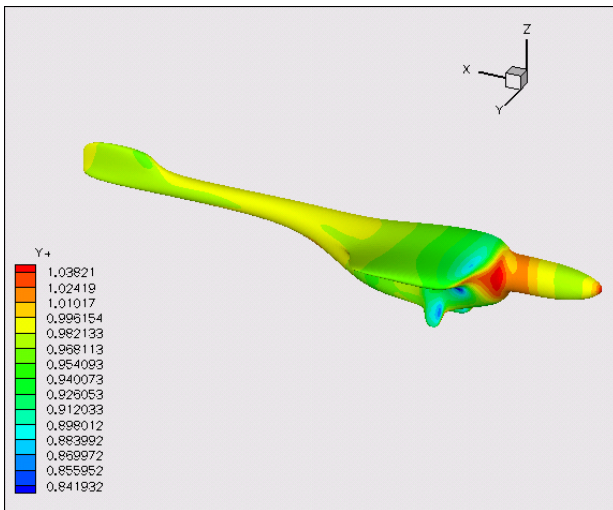


Figure 7: Computed y^+ distribution for MTR-SD fuselage with streamlined fuel tank at nominal conditions (Mach=0.325, $Re=4.2M/m$).

$Re=4.2M/m$

Cd	Cd-p	Cd-f	FPA (sq meter)
0.06124	0.03104	0.03020	0.05177

Table 3: Computed drag coefficients for MTR-SD fuselage with streamlined fuel tank. Equivalent flat plate area (FPA) calculation is for the half geometry.

For the cargo pod flow calculations, the Mach number was set to 0.325 and the Reynolds number was set to the same value as previously (4,224,901 per meter). Convergence of NSU3D for this case was similar to that reported for the fuselage geometry. Figure 8 depicts the surface pressure contours for this case, and Figure 9 shows the Mach contours on the two symmetry planes,

indicating that the flow is predominantly attached over the entire surface of the pod. Figure 10 illustrates the y^+ value computed for the spacing of the first cell height at the wall over the surface of the cargo pod, demonstrating that the normal resolution of this mesh is within the acceptable range of $y^+ < 1$, for accurate drag prediction. The drag values (pressure and friction drag) are given in Table 4 for this case, using a reference area of 0.541179 square meters in the definition of these force coefficients.

Based on previous experience and validation with NSU3D, and based on the grid resolution used in this study, the drag values reported for both geometries can be considered to be reliable and accurate.

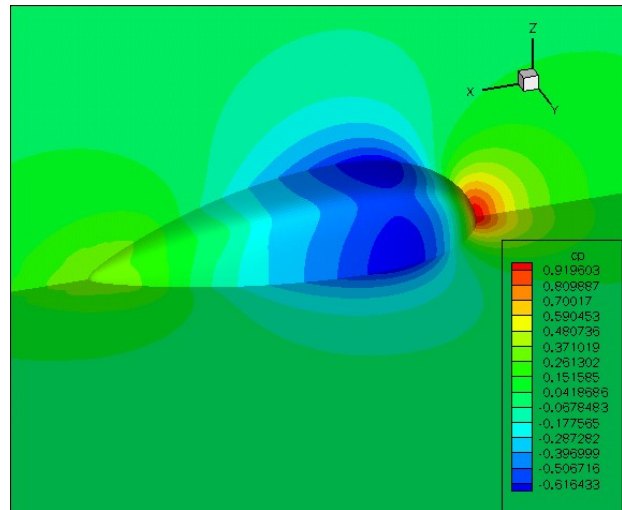


Figure 8: Computed pressure coefficient distribution on MTR-SD streamlined cargo pod at nominal conditions (Mach=0.325, $Re=4.2M/m$).

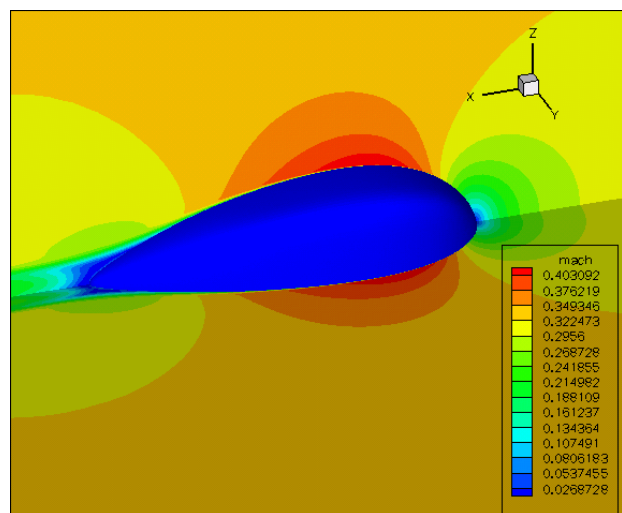


Figure 9: Computed Mach number distribution on symmetry planes for MTR-SD streamlined cargo pod at nominal conditions (Mach=0.325, $Re=4.2M/m$)

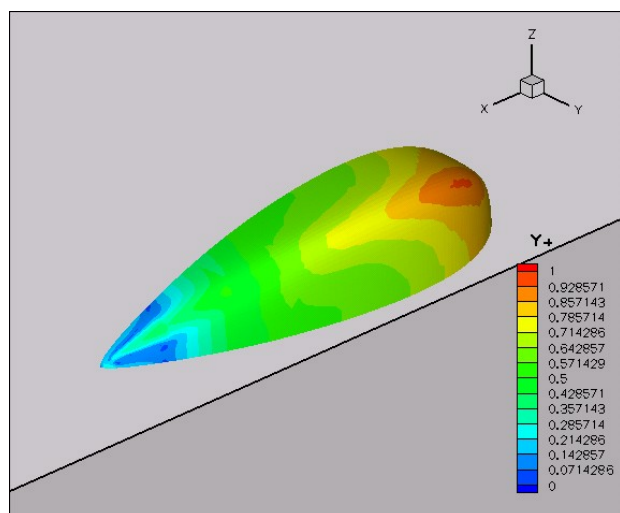


Figure 10: Computed y^+ distribution for MTR-SD streamlined cargo pod at nominal conditions ($Mach=0.325$, $Re=4.2M/m$).

A summary of MTR-SD drag in airplane mode, both with and without incorporating the CFD drag calculations is provided in Table 5. The first column tabulates the values reported by BTC in the MTR-SD final report; the second column tabulates the values calculated by BHTI using their 1st order drag estimation techniques, and the third column shows the differences between the BTC estimates and the BHTI estimates. The two high risk items identified by BHTI are shown in red, and these items were the subject of the streamlining and CFD assessment discussed above. The column titled “CFD w/BHTI” duplicates BHTI results with changes to only

A/P Mode						
Item	Baldwin	BHTI	Δf_e	Comment	CFD w/ BHTI	Δf_e
Spinner/Tailboom	0.273	0.459	0.186	(included with fuel tank)	0	-0.273
Nacelle/Fuel Tank	2.786	4.076	1.290	(engine area extracted)	1.114	-1.672
Wing Panels	1.134	1.670	0.536		1.670	0.536
Alighting Gear	0.035	0	-0.035	(not deployed in fwd flight mode)	0	-0.035
V & H Tail	0.500	0.263	-0.237		0.263	-0.237
Struts	0.566	0.364	-0.202		0.364	-0.202
Fuselage fairings	0.013	0	-0.013	(included in fuselage)	0	-0.013
Fuselage	0.944	1.287	0.343	(frontal only)	0.716	-0.228
Fuse V-Tails	0.168	0.239	0.071		0.239	0.071
Interference	1.284	0	-1.284	(included in each component)	0	-1.284
sub totals	7.704	8.358	0.654		4.366	-3.338
Protuberances	0	0.836	0.836	(% component total)	0.437	0.437
Trim	0	0.500	0.500	(estimated)	0.500	0.500
Momentum	0	0.383	0.383	(xsmn cooling, eng, etc.)	0.383	0.383
fe A/P MODE =	7.70	10.08	2.37		5.686	-2.018

Table 5: BHTI drag assessment of the MTR-SD in airplane mode, with adjustments incorporating CFD results.

Cd	Cd-p	Cd-f	FPA (sq meter)
0.03071	0.01045	0.02026	0.01662

Table 4: Computed drag coefficients for MTR-SD streamlined cargo pod. Equivalent flat plate area (FPA) calculation is for the quarter geometry.

the three values highlighted in green reflecting the effect of streamlining and the resulting CFD drag calculation. The final column shows the differences between the original BTC estimates this BHTI adjusted calculation. Note that the fuselage listed in this table is also known as the cargo pod.

Helicopter Mode Power Requirements

Preliminary design, 1st order performance models were utilized with the predicted drag levels and provided engine performance to evaluate the MTR performance in hover and in helicopter mode forward flight.

Hover-out-of-ground-effect (HOGE) calculations were performed utilizing a modified blade-annulus model with empirical corrections for co-axial rotors. The model includes: tip loss as a function of thrust coefficient, a three-term airfoil polar, blade lift-curve corrections for blade aspect ratio, compressibility, and optimum rotor twist. The download was matched to that reported in MTR-SD final report. The results for the specified condition are listed in Table 6 as well as the assumed losses. The values are within 1-2% of those predicted by

Power Summary	
$\eta_{xsmn MR} = 0.950$	HP _{MR} = 1,494.2
$\eta_{xsmn co-box} = 1.000$	$\delta HP_{MR \times smn}^4 =$ 78.6
$\eta_{inst}^5 = 0.925$	$\Delta HP_{ACC} =$ 25
	$\delta HP_{ACC}^4 =$ 0.0
	ESHP _{ins} = 1,597.8
	$\delta HP_{inst} =$ 129.6
	ESHP _{unins} = 1,727.4
	Referred⁶ HP_{SL unins} = 1,727.4

Table 6: Hover out of ground effect at sea level ISA.

a separate Comprehensive Program for Theoretical Evaluation of Rotorcraft, (COPTER) analysis.

Helicopter mode forward flight analysis was performed using a classic rotorcraft component analysis. The power required is separated into rotor power, anti-torque power (if required) and parasite power. The rotor power is further separated into induced and profile power.

The rotor power required includes correction to the profile power for retreating blade stall, compressibility, and Mach drag divergence, and correction to the induced power for non-uniform downwash and a free wake correction. The analysis is a point performance approach that utilizes a constant (assumed) trim drag (included in the drag analysis). The speed power polar for the MTR-SD at sea-level ISA for helicopter mode forward flight with the wings fully deployed is shown in Figure 11. As noted, the mast angle was assumed to be "0" degrees. The hover point is included for reference. These forward flight results compare favorably to an independent COPTER analysis at zero mast incidence.

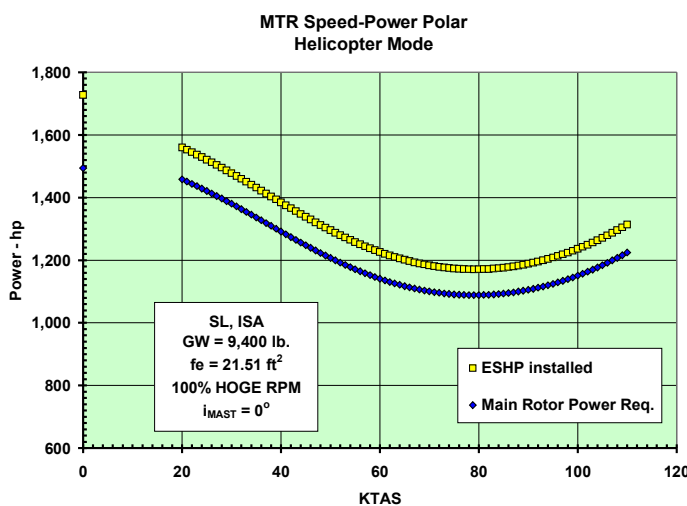


Figure 11: MTR-SD helicopter mode speed power polar.

Airplane Mode Propulsive Efficiency

The BHTI propeller/proporotor model used in the analysis of the MTR-SD is a combination of a series of "classical", "fundamental" propeller analysis models. It includes:

- L. Prandtl's disk actuator momentum/kinetic energy propeller theory
- S. Drezewiecki's original blade-element-momentum theory,
- S. Goldstein's vortex theory (multi-sheet wake vs. H. Glauert's merged single sheet)
- T. Theodorsen's application of Prandtl-Glauert compressibility corrections, and
- Empirical corrections for blade stall, Mach drag divergence (Mdd), lift degradation at Mdd, and contra-rotating propeller interactions

This specific model has been correlated to measured flight test data (i.e. measured torques and RPM's at the hub) via:

- NOAA /NSSL's Beech King Air icing research aircraft (at the University of Wyoming),
- Edwards AFB Flight Test Center for icing test of the MU2 and the ATR-72 for the FAA, and
- independent testing of the DeHavilland DH-6 Twin Otter aircraft

In all cases, the predicted results were within +/-1% of the measured data. Additionally, the model has been used at BHTI to predict the performance of tiltrotor vehicles in the airplane mode and correlated with COPTER modeling. Comparisons of the two predictions were, again, within 1-2% up to speeds approaching 320 knots true air speed, at which time the model produces optimistic values for propulsive efficiency. Above that speed, Mach & compressibility interactions for the helical tip Mach numbers seen in tiltrotors appear to govern the efficiency. This is the propeller model presently in use at BHTI in the conceptual/preliminary design organization and was utilized to perform the evaluation of the performance of the MTR-SD.

The major difference in the results of this analysis as compared to the MTR-SD final report (67% vs. 71%) lies in the assumed values used for the incompressible mean blade drag coefficient (integrated value). The propeller efficiency is sensitive to the value assumed for the mean blade drag coefficient. Based on BHTI experience, the significant "drag buckets" that are demonstrated in 2-D airfoil wind tunnel test are rarely achieved in flight test and almost

never achieved in production vehicles due to manufacturing issues. To this end, for initial configuration analysis, BHTI normally does not utilize the minimum drag coefficient of the "bucket" as demonstrated in 2-D testing. As a general "best practice", "smoothed" polar data above the "bucket" is used for performance predictions as obtaining "bucket" results has not been demonstrated in practice.

Figure 12 shows the variation of the MTR-SD proprotor propulsive efficiency in forward flight for the given blade geometry. The flight conditions and vehicle specifics are included in the chart. The results include an increase in propulsive efficiency of approximately 1.5% due to the positive interaction of the coaxial propeller configuration (based on NACA tandem propeller test results). A range of 2D wind tunnel values for the minimum blade drag coefficient of VR7 airfoil family in the "bucket" region are included on the left margin of the chart for reference. Basically, for the MTR-SD proprotor to achieve the propulsive efficiency value of 71%, the mean blade drag coefficient would need to be 0.00858. The value utilized in this analysis was 0.011 (for the 67% propulsive efficiency result) and was determined from the integration of the local blade drag coefficient as a function of its local angle-of-attack and loading along the blade radius.

Also included in Figure 12 is the effect of slowing the proprotor in forward flight. The 84% value was selected to be representative of conventional tiltrotors for comparative purposes. This is generally accomplished via varying the speed of the power turbine relative to the core gas generator. The significant difference in propulsive efficiency between the MTR-SD and a conventional tiltrotor is due to the design speed and twist distribution of the MTR-SD proprotor.

The BHTI propulsive efficiency analysis excludes any residual thrust contribution due to the pair of pod mounted turboshaft engines. For a reference installation at cruise operating conditions, the combination of turboshaft engines and enclosing nacelle would produce small positive thrust, which has been verified through CFD analyses.

Flight Dynamics

Evaluation of the MTR-SD flight dynamics was carried out using the BHTI Comprehensive Program for Theoretical Evaluation of Rotorcraft, (COPTER) [16]. COPTER is a general purpose flight simulation program capable of analyzing an entire rotorcraft in level or maneuvering flight. COPTER can compute rotorcraft

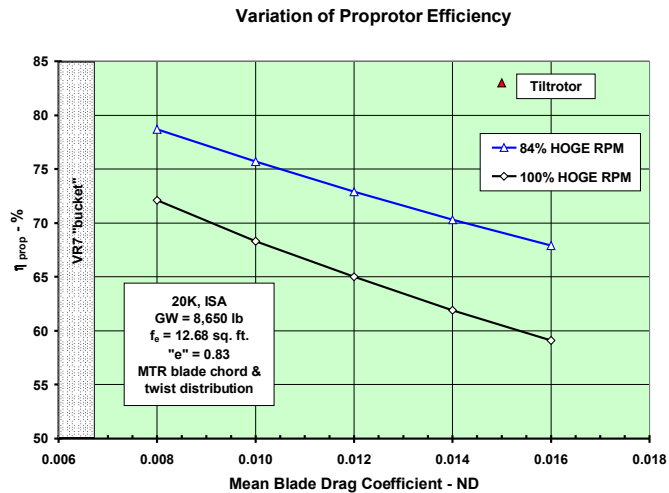


Figure 12: MTR-SD proprotor forward flight propulsive efficiency.

trim, performance, stability derivatives, control powers, blade loads and vibrations for any type of flight condition.

The program can model the major dynamic components of a rotorcraft. That includes up to four rotors and pylons, wing, elevators and fins, elastic airframe, and the six rigid body degrees of freedom. Rotor dynamics is normally modeled by Myklestad computed mode shapes and natural frequencies. Rotor aerodynamics, airframe aerodynamics and control system components are also modeled.

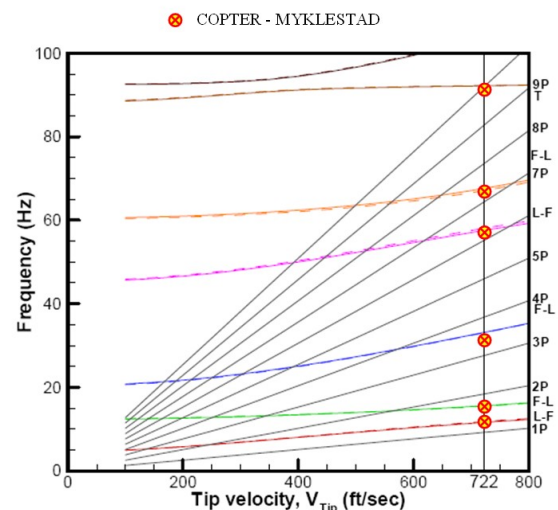


Figure 13: Blade frequency placements from MTR-SD final report compared to COPTER results.

Flight dynamics of the MTR-SD was studied for the aircraft in following conditions and configurations:

1. Hover with wings un-deployed, sea level standard atmosphere (SLS)
2. Helicopter mode, 60 kts forward flight, wings deployed, SLS
3. Airplane mode, 200 kts, 20,000 ft, standard day

Inputs to the COPTER simulation were obtained from the MTR-SD final report and from the CAMRAD input data that accompanied the report.

The rotor structural properties and twist given in MTR-SD final report for both the upper and lower rotors were incorporated into the COPTER analysis. A comparison of the resultant rotor dynamics model used by COPTER with the rotor dynamics model use by the CAMARAD program is shown in Figure 13. The figure shows that both simulations predicted essentially the same modal frequencies to within 0.1 per rev.

Agreement between the two programs was found for the mode shapes as well as frequency placements. For this preliminary assessment of the MTR's flight dynamics, only the first two rotor modes are of critical importance, only the first two rotor modes are of critical importance. The higher frequency modes are more important when looking into loads and vibrations issues. Figures 14 and 15 compare the first two mode shapes computed by these two programs for the upper rotor. They are in agreement on the shape of the out of plane and inplane components

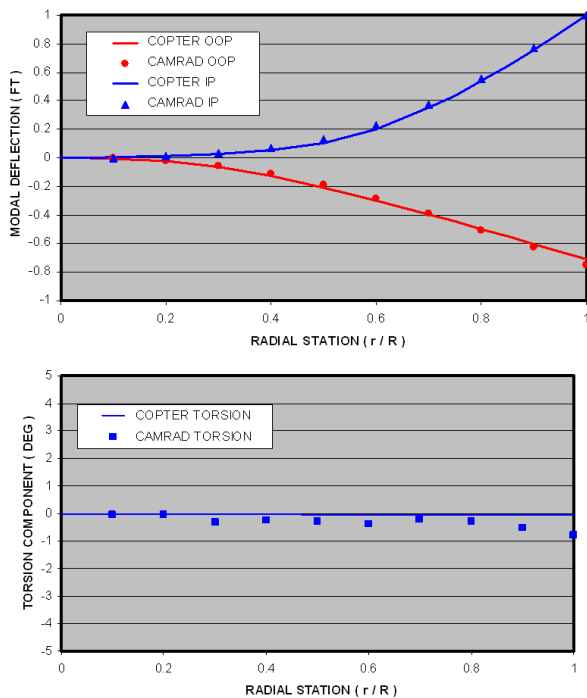


Figure 14: First mode shape (L-F) comparison between MTR-SD final report and COPTER results.

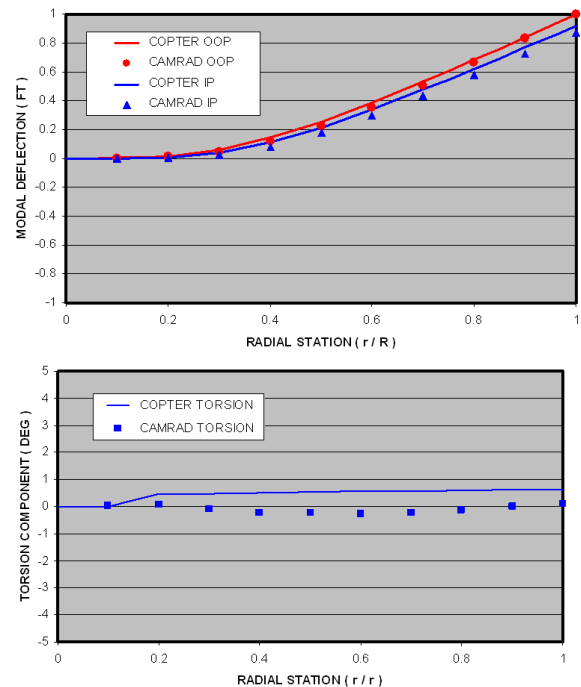


Figure 15: Second mode shape (F-L) comparison between MTR-SD final report and COPTER results.

of the modes. There is a slight disagreement on the amount of the torsion coupling in the two modes. In each of the figures the mode shapes are normalized to the same one foot of tip deflection. For the first L-F (lag-flap) mode that means one foot of inplane tip deflection as can be seen in Figure 14 and one foot of out of plane tip deflection for the second F-L mode shown in Figure 15.

Inputs to describe the aircraft and rotor aerodynamics came from data presented in MTR-SD final report as well as from data generated in the BHTI drag assessment section above. Airfoil tables representative of the VR-12 series of airfoils used on the rotor came from the Bell Helicopter library of airfoil data tables. Wing and

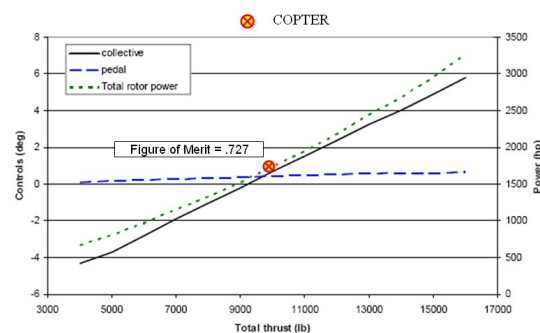


Figure 16: Hover power required comparison between MTR-SD final report and COPTER results.

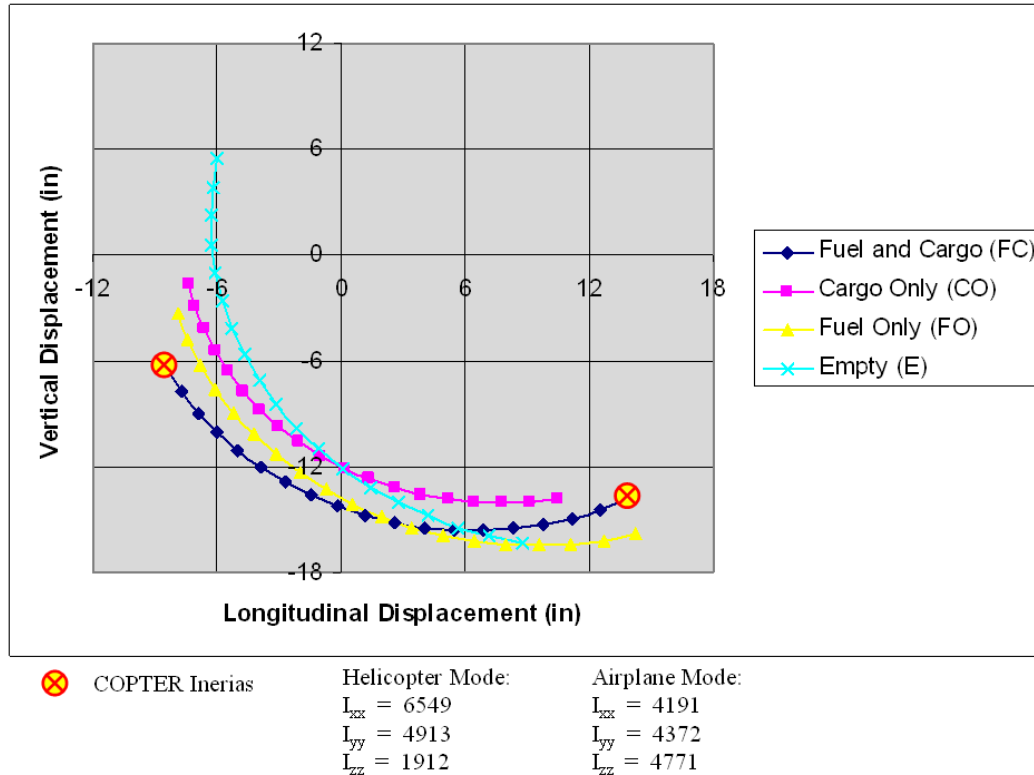


Figure 17: System level CG referenced to the tilt-hinge location; and system level inertias.

stabilizer aerodynamics were modeled using existing Bell data tables suitably modified to represent the appropriate aerodynamic surfaces given in the MTR-SD final report.

Performance computed using this COPTER model of the MTR-SD was found to be in good agreement with the performance presented above and with the performance numbers computed by CAMRAD. Figure 16 shows the agreement between COPTER and CAMRAD for hover predictions of thrust and power.

Weight and center of gravity information for these simulations is shown in Figure 17 which was taken directly from the MTR-SD final report. Aircraft inertias shown were obtained from the spreadsheet of component weights and inertias which accompanied the CAMRAD input data. The inertias presented in the figure do not include the weight and moment arm of the payload and represent only the basic airframe inertias.

In COPTER, the stability analysis can include the following degrees of freedom:

- Six rigid body modes (total rotorcraft)
- Eight elastic fuselage modes
- Fore-and-aft and lateral flapping for four rotors
- Three other elastic blade modes for four rotors

At this stage of the MTR-SD assessment there is no need to consider the impact of elastic airframes and rotors on the vehicle's flight dynamics. It will be sufficient for this preliminary analysis to consider only the six rigid body degrees of freedom. Since the time constant for the rotor is well removed from the airframe's dynamic response the rotor dynamics can be absorbed into these six equations using the classical quasi-static assumption. This assumption eliminates the blade motions as a separate degree of freedom and instead treats the rotor as a source of forces and moments that responds instantaneously to changes in flight conditions.

The COPTER stability analysis may be performed for a trimmed flight condition or for specified times during a maneuver. The three matrices (mass, damping and stiffness) generated by the analysis can then be used as input to other analyses. The quasi-static rotor analysis uses a harmonic balance method for solving the rotor's equations of motion.

Table 7 presents the six equations of motion needed to model the MTR in hover. The mass matrix is given in terms of slugs mass and slug-ft² inertia. Translational rates are given in ft/sec while angular rates are in radians/sec. Control powers for this example are given in Table 8.

The control powers in hover are given in terms of pounds of force and ft-lbs of moment. The control deflections are expressed in terms of inches of pilot stick motion. The actual input to the rotor is dependent on how the stick is attached to the swashplate and then to the blade pitch. The collective, fore/aft (F/A), and lateral riggings can be somewhat arbitrary. In the case of the MTR-SD in hover the control riggings are:

- Collective rigging = 10 degrees of steady root pitch / one inch of collective stick
- F/A rigging = 2 degrees of A1s / one inch of F/A stick
- Lateral rigging = 2 degrees of B1s / one inch of Lateral stick

Due to the nature of anti-torque control designed into the MTR-SD transmission the pedal was not rigged to rotor blade pitch. Instead it was connected to a pure torque. The amount of torque provided by pedal inputs will need to be adjusted to represent the controls and transmission of the final MTR-SD design. For now the pedal was set to give 4000 ft-lbs of anti-torque per one inch of pedal input.

Since the MTR-SD rotor natural flapping frequency is well above once per revolution the nature of the rotor controls shown above has been changed dramatically over that of a normal helicopter. Because the flapping frequency of a typical helicopter is around once per revolution the fore and aft flapping of a typical helicopter is accomplished by changing B1s and the lateral flapping is controlled by A1s. As can be seen above these two blade feathering angles, A1s and B1s have swapped functions.

Table 9 presents the six equations of motion needed to model the MTR-SD in helicopter mode at 60 knots forward speed with the tailboom deployed. Like the hover case above, the mass matrix is given in terms of slugs mass and slug-ft² inertia and the translational rates are given in ft/sec while angular rates are in radians/sec.

The control powers for the MTR-SD in helicopter mode with the tailboom deployed are given in Table 10. Again control power is expressed in terms of pounds of force and ft-lbs of moment. The control deflections are also given in terms of inches of pilot stick motion. In the case of the MTR-SD in this configuration and condition the control riggings are:

- Collective rigging = 10 degrees of steady root pitch / one inch of collective stick
- F/A rigging = (2 degrees of A1s / one inch of F/A stick) + (4.0 degrees of elevator deflection / one inch of F/A stick)

- Lateral rigging = 2 degrees of B1s / one inch of Lateral stick

Again due to the nature of anti-torque control designed into the MTR-SD transmission the pedal was not rigged to rotor blade pitch. It was again connected to a pure torque as it was in hover. However, in the case of flight at 60 knots the pedal was also connected to the rudder on the vertical fin with a rigging of 8 degrees of rudder deflection per inch of pedal input. So the control power for the pedal represents the combination of the two.

Like the pedal the F/A stick also has more than one connection. Besides the normal connection to rotor cyclic the F/A stick is also rigged to move the elevator on the horizontal stabilizer. Note also that the lateral stick could have also been rigged to move the wing's flaperons so they could be used as ailerons. For the purposes of this study the flaperons were not used in this manner. However, in Table 11 the control power of each aerodynamic surface was computed per one degree of flap deflection so that the effectiveness of the wing flaperons can be included if so desired.

In the figure surface 1 represents the portion of the right wing that is not directly in the rotor downwash field. Surface 2 represents the portion of the left wing that is not in the rotors wakes. Meanwhile the column under the heading RIGHT W represents the portion of the right wing that is directly under the rotors wake and the control powers listed under the heading LEFT W represent the portion of the left wing that is in the rotors wakes.

Surface 3 is the horizontal stabilizer and breaks out the contribution of the elevator to the F/A control power from the contributions of the rotor system. Surface 4 is the vertical fin and allows the contribution of the rudder to be separated from the MTR-SD anti-torque device.

Table 12 presents the six equations of motion needed to model the MTR-SD in airplane mode at 200 knots forward speed and 20,000 feet. Like all of the previous cases, the mass matrix is given in terms of slugs mass and slug-ft² inertia and the translational rates are given in ft/sec while angular rates are in radians/sec.

The control powers for the MTR-SD in airplane mode are given in Table 13. Again control power is expressed in terms of pounds of force and ft-lbs of moment. The control deflections are also given in terms of inches of pilot stick motion. In the case of the MTR in the airplane configuration and flying at 200 knots the control riggings are:

- Collective rigging = 10 degrees of steady root pitch / one inch of collective stick
- F/A rigging = 4.0 degrees of elevator deflection / one inch of F/A stick

----- MASS MATRIX -----						
	U DOT	W DOT	Q DOT	V DOT	P DOT	R DOT
X-FORCE	292.17	0.0000	0.0000	0.0000	0.0000	0.0000
Z-FORCE	0.0000	292.17	0.0000	0.0000	0.0000	0.0000
PITCH MOMENT	0.0000	0.0000	4913.0	0.0000	0.0000	0.0000
Y-FORCE	0.0000	0.0000	0.0000	292.17	0.0000	0.0000
ROLL MOMENT	0.0000	0.0000	0.0000	0.0000	6549.0	0.0000
YAW MOMENT	0.0000	0.0000	0.0000	0.0000	0.0000	1912.4

----- DAMPING MATRIX -----						
	U	W	Q	V	P	R
X-FORCE	13.609	1.8602	-11.542	-6.1834	-47.559	1.1140
Z-FORCE	-11.865	86.568	66.193	3.5753	69.453	20.767
PITCH MOMENT	-172.75	48.624	-40.220	47.352	258.17	-12.519
Y-FORCE	6.9816	0.19234	-65.495	12.974	54.260	28.639
ROLL MOMENT	33.507	15.038	-407.31	133.53	-763.97	243.59
YAW MOMENT	19.815	33.862	-184.36	-24.254	-33.508	1106.0

----- STIFFNESS MATRIX -----						
	X	Z	THETA	Y	PHI	PSI
X-FORCE	0.0000	0.0000	9399.4	0.0000	0.0000	0.0000
Z-FORCE	0.0000	0.0000	-102.75	0.0000	81.305	0.0000
PITCH MOMENT	0.0000	0.0000	0.0000	0.0000	0.0000	0.0000
Y-FORCE	0.0000	0.0000	-0.88880	0.0000	-9399.1	0.0000
ROLL MOMENT	0.0000	0.0000	0.0000	0.0000	0.0000	0.0000
YAW MOMENT	0.0000	0.0000	0.0000	0.0000	0.0000	0.0000

Table 7: Mass, damping and stiffness matrices representing the MTR-SD in hover.

CONTROL PARTIAL DERIVATIVE MATRICES				
PILOT CONTROLS				
	COLLECTIVE	F/A CYCLIC	LAT CYCLIC	PEDAL

POUNDS/INCH				
X-FORCE	-6.162	96.76	-73.41	-0.4507E-04
Y-FORCE	-9.234	75.96	88.07	-0.1695E-04
Z-FORCE	-0.1339E+05	-206.5	-3.433	0.5425E-03
FOOT-POUNDS/INCH				
YAW MOM	-3302.	-33.65	-54.56	4000.
PITCH MOM	-8090.	-1884.	-72.73	0.6874E-03
ROLL MOM	598.8	-37.18	1761.	-0.4069E-03

Table 8: Control power matrices for the MTR-SD in hover.

----- MASS MATRIX -----						
	U DOT	W DOT	Q DOT	V DOT	P DOT	R DOT
X-FORCE	292.17	0.0000	0.0000	0.0000	0.0000	0.0000
Z-FORCE	0.0000	292.17	0.0000	0.0000	0.0000	0.0000
PITCH MOMENT	0.0000	0.0000	5217.0	0.0000	0.0000	0.0000
Y-FORCE	0.0000	0.0000	0.0000	292.17	0.0000	0.0000
ROLL MOMENT	0.0000	0.0000	0.0000	0.0000	4266.0	0.0000
YAW MOMENT	0.0000	0.0000	0.0000	0.0000	0.0000	5539.0

----- DAMPING MATRIX -----						
	U	W	Q	V	P	R
X-FORCE	2.8383	-14.027	-2239.9	-1.1586	-27.684	18.352
Z-FORCE	65.184	268.49	-28967.	-3.3213	-133.84	-8.1846
PITCH MOMENT	220.47	162.10	10179.	27.676	855.28	-201.88
Y-FORCE	0.52054	0.19428	11.645	27.838	2305.9	29311.
ROLL MOMENT	-10.755	-10.142	139.16	167.63	10532.	-5532.2
YAW MOMENT	1.6063	12.490	109.80	-206.08	1598.4	4479.0

----- STIFFNESS MATRIX -----						
	X	Z	THETA	Y	PHI	PSI
X-FORCE	0.0000	0.0000	9374.2	0.0000	0.0000	0.0000
Z-FORCE	0.0000	0.0000	-695.62	0.0000	88.916	0.0000
PITCH MOMENT	0.0000	0.0000	0.0000	0.0000	0.0000	0.0000
Y-FORCE	0.0000	0.0000	-6.5984	0.0000	-9373.8	0.0000
ROLL MOMENT	0.0000	0.0000	0.0000	0.0000	0.0000	0.0000
YAW MOMENT	0.0000	0.0000	0.0000	0.0000	0.0000	0.0000

Table 9: Stability matrices representing the MTR-SD in helicopter mode at 60 knots.

CONTROL PARTIAL DERIVATIVE MATRICES				
PILOT CONTROLS				
	COLLECTIVE	F/A CYCLIC	LAT CYCLIC	PEDAL

POUNDS/INCH				
X-FORCE	-1026.	13.72	-14.01	-2.198
Y-FORCE	-161.7	16.96	81.32	-92.36
Z-FORCE	-0.1335E+05	-98.93	40.64	0.5425E-03
FOOT-POUNDS/INCH				
YAW MOM	172.3	-114.1	-330.2	5473.
PITCH MOM	0.2010E+05	-3320.	-246.5	6.953
ROLL MOM	-1934.	-39.70	1747.	-292.1

Table 10: Primary control power matrices for the MTR-SD at 60 knots.

	SURFACE 1	SURFACE 2	SURFACE 3	SURFACE 4	RIGHT W	LEFT W

POUNDS/DEGREE						
X-FORCE	1.271	1.271	-8.759	-0.7902	-5.655	-5.655
Y-FORCE	-0.6104E-04	-0.6104E-04	-0.6104E-04	-11.55	-0.6104E-04	-0.6104E-04
Z-FORCE	-16.00	-16.00	-28.76	-0.8545E-03	-5.628	-5.628
FOOT-POUNDS/DEGREE						
YAW MOM	-16.56	16.56	-0.5264E-03	184.2	34.29	-34.27
PITCH MOM	-16.59	-16.59	-408.3	2.499	59.63	59.63
ROLL MOM	-208.5	208.5	-0.2441E-03	-36.53	-59.03	59.00

Table 11: Control power of the individual fixed aerodynamic surfaces.

----- MASS MATRIX -----						
	U DOT	W DOT	Q DOT	V DOT	P DOT	R DOT
X-FORCE	292.17	0.0000	0.0000	0.0000	0.0000	0.0000
Z-FORCE	0.0000	293.23	0.0000	0.0000	0.0000	0.0000
PITCH MOMENT	0.0000	13.921	4372.0	0.0000	0.0000	0.0000
Y-FORCE	0.0000	0.0000	0.0000	292.17	0.0000	0.0000
ROLL MOMENT	0.0000	0.0000	0.0000	0.0000	4191.0	0.0000
YAW MOMENT	0.0000	0.0000	0.0000	0.0000	0.0000	4771.0
----- DAMPING MATRIX -----						
	U	W	Q	V	P	R
X-FORCE	11.156	-18.385	-472.46	0.12853E-02	4.0878	3.3211
Z-FORCE	57.817	264.12	-97888.	-0.67667E-01	1.5931	-14.649
PITCH MOMENT	-35.329	142.59	15299.	-11.314	-285.28	-299.44
Y-FORCE	-0.71089E-03	0.60953E-01	-13.324	70.675	487.09	98490.
ROLL MOMENT	-3.6984	1.3593	-2.0092	258.69	18927.	-5386.1
YAW MOMENT	-0.19599	-11.195	308.99	-80.720	-788.10	7197.7
----- STIFFNESS MATRIX -----						
	X	Z	THETA	Y	PHI	PSI
X-FORCE	0.0000	0.0000	9400.0	0.0000	0.0000	0.0000
Z-FORCE	0.0000	0.0000	-27.764	0.0000	-3.2883	0.0000
PITCH MOMENT	0.0000	0.0000	0.0000	0.0000	0.0000	0.0000
Y-FORCE	0.0000	0.0000	0.97125E-02	0.0000	-9400.0	0.0000
ROLL MOMENT	0.0000	0.0000	0.0000	0.0000	0.0000	0.0000
YAW MOMENT	0.0000	0.0000	0.0000	0.0000	0.0000	0.0000

Table 12: Stability matrices representing the MTR-SD in airplane mode at 200 knots.

CONTROL PARTIAL DERIVATIVE MATRICES				
PILOT CONTROLS				
	COLLECTIVE	F/A CYCLIC	LAT CYCLIC	PEDAL

POUNDS/ INCH				
X-FORCE	0.1374E+05	-160.2	0.2131	0.8774E-01
Y-FORCE	0.6065E-01	0.000	0.000	-549.8
Z-FORCE	10.82	-748.2	-0.1085E-02	0.000
FOOT-POUNDS/ INCH				
YAW MOM	1.635	0.000	-27.82	7262.
PITCH MOM	-0.2015E+05	-8659.	-0.4888	-0.4416
ROLL MOM	887.9	0.000	9420.	-2766.

Table 13: Control power matrices for the MTR-SD at 200 knots.

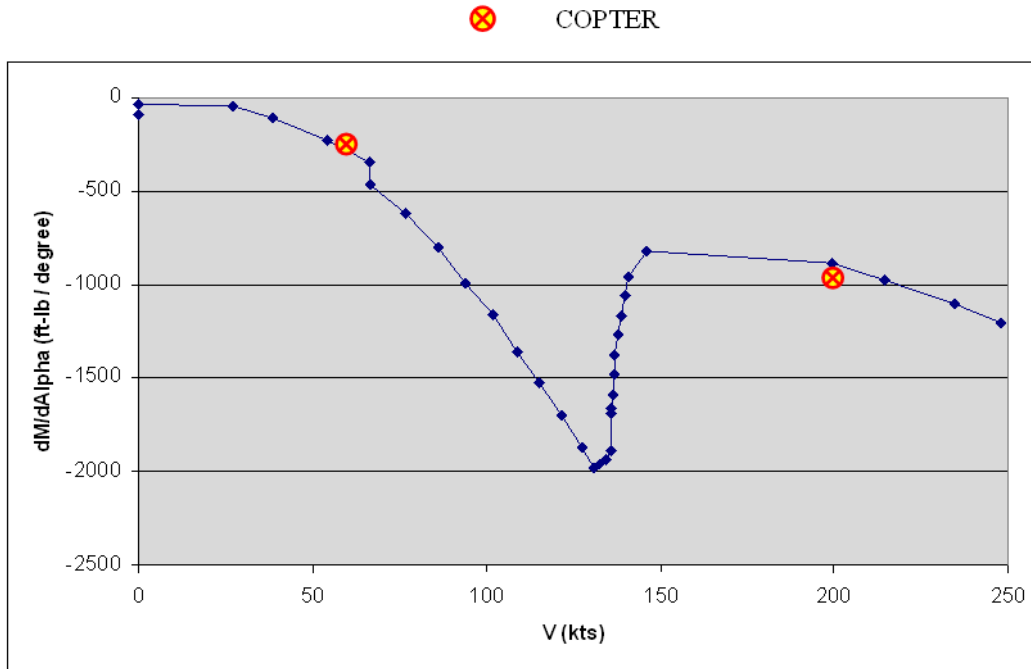


Figure 18: Change in aircraft pitching moment for a change in aircraft pitch angle at maximum gross weight; comparison between MTR-SD final report and COPTER results.

- Lateral rigging = 4.0 degrees of differential flaperon / one inch of LAT stick
- Pedal rigging = 8.0 degrees of rudder deflection / one inch of Pedal

COPTER computed results were compared to what little stability and control data was made available in MTR-SD final report. A comparison of the COPTER computed C_m -alpha with the C_m -alpha reported in the MTR-SD final report is presented in Figure 18. The comparison suggests that the preceding models may be used with confidence in designing the preliminary control laws.

Airplane Mode Cruise Performance

The forward flight evaluation was performed by BHTI using the BHTI generated drag predictions. Subsequently, BTC adjusted the BHTI performance results to incorporate the CFD drag calculations. As a point of reference, the BHTI airframe lift-to-drag ratio (L/D) was also adjusted to the original drag estimates of the MTR-SD final report. Figure 19 shows the airframe L/D as computed by BHTI based on their 1st order drag assessment. Also shown are airframe L/Ds

based on the parasitic drag of the MTR-SD final report (Original), and based on the BHTI parasitic drag adjusted by the streamlined CFD results (CFD). These revised L/Ds were computed by replacing the BHTI computed parasitic drag with the original and CFD adjusted parasitic drags, leaving all other calculations unchanged.

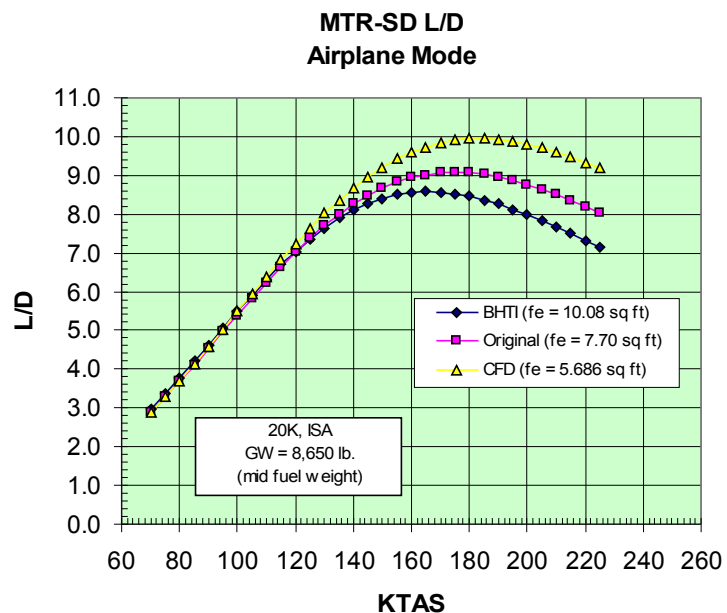


Figure 19: MTR-SD airframe L/D.

MTR-SD Speed-Power Polar Airplane Mode

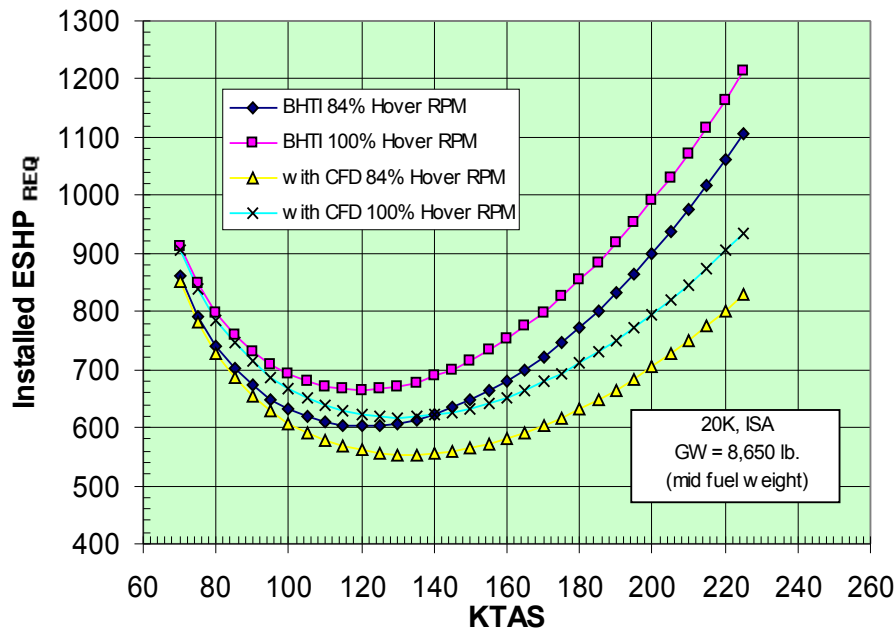


Figure 20: MTR-SD speed-power polar.

BHTI used the mid-fuel weight for the performance evaluation to provide an approximation of the Breguet dry tank range at the specified cruise altitude. Both 100% and 84% HOGE RPM data were included to demonstrate the effect of a slowed propotor in forward flight.

The speed-power polar for the vehicle at the 20,000 feet ISA cruise flight condition is shown in Figure 20 while the L/D effective (L/De) is shown in Figure 21. The results are shown both with and without the CFD drag analysis adjustment.

Using 100% HOGE RPM for the forward flight mode the results indicate, for the specified engine lapse, that two engines will be required to maintain 200 knote true air speed (KTAS) cruise at 20k ISA conditions (89.9% of the twin engine power available is required using the BHTI 1st order drag estimate). The 0.99SRmax velocity is approximately 180 KTAS with a 0.99SRmax value of 0.41 nm/lbf. This would yield a dry tank range at altitude of approximately 740nm when factoring in the CFD analysis, or 615 nm when not incorporating the CFD analysis, without any allowances for take-off (T/O), climb, descent, etc.

Using 84% HOGE RPM for the forward flight mode yields a 200 KTAS cruise at 20k ISA conditions on only 79% power available. The 0.99SRmax velocity is approximately 187 KTAS with a 0.99SRmax value of 0.45 nm/lbf. This would yield a dry tank range at altitude of approximately 845nm when factoring in the CFD analysis, or 675 nm when not incorporating the CFD analysis, without any allowances for T/O, climb, descent, etc.

BHTI reported that the range computed exclusive of the CFD results is somewhat less than the 782 nm (with climb, etc.) predicted in the MTR-SD final report and can be contributed to two factors: a) the assessed drag level of the vehicle and, b) the propulsive efficiency of the co-axial propotor in forward flight. The MTR-SD final report shows propulsive efficiency utilizing the

hover RPM of the rotor of 0.71 for the 200 kts cruise condition while Bell's calculations yield a value of approximately 0.67. This propulsive efficiency difference accounts for approximately 6-7% of the variation while the drag difference account for the remaining range/speed

MTR-SD L/D_e Airplane Mode

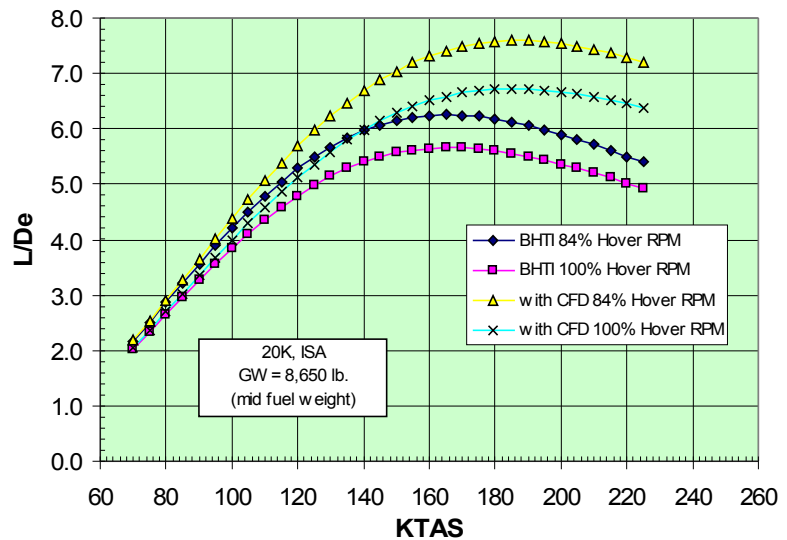


Figure 21: MTR-SD L/D effective (L/De).

differences. BHTI reports that both of these factors can be improved upon with additional design efforts, which was subsequently proven to be true for drag.

As mentioned above, it was after BHTI delivered their report that the streamlined bodies were subjected to an authoritative CFD analysis. The streamlining and CFD analysis resulted in improved drag performance. The CFD adjusted airplane mode performance is consistent with the MTR-SD final report numbers. Further improvements in range due to proprotor design changes are also potentially feasible based on the BHTI results reported above.

Results and Discussion

The results to be drawn from the preceding section of this paper are significant. All of the key innovative features of the MTR aircraft architecture have been built and tested at an RC scale. Furthermore, these features have been integrated into the design of a functional demonstrator that has already performed a hover test, and is suitable for integrated testing of these key innovative features. Independent authorities have assessed the 9,400 pound gross weight MTR-SD [2, 3] design, and have essentially concurred with all quantified facets of the aircraft to within a reasonably small margin of error in all categories examined: weight, drag, hover performance, propulsive efficiency, flight dynamics, and cruise performance. Furthermore, these results validate the assumptions of the original MTR mission performance concept studies reported in 2004 and 2005 [17, 18, 19].

Validation of key MTR features

The three key features validated through RC scale hardware flight testing are the aerodynamically deployed wing panels, the pitch axis suspended cargo pod, and the tilting rotor. The fact that functional wing hinges with remotely controlled locking and unlocking mechanism have been designed and built proves the existence of a practical mechanism. The fact that a repeatable and controllable flight procedure was developed for commanding the deployment of the wing panels, locking the wing panels when they fully deploy, and then commanding the unlocking of the wing panels for recovery and landing shows that a procedure for operating the wing panels exists. This is significant in that it is apparently the first time ever that a VTOL aircraft has been operated with aerodynamically deployable and locking wing panels. This technique eliminates the aerodynamic download that would otherwise be caused by the wing panels in the rotor wake. Furthermore, the pilot found that the aircraft was much more controllable in hover with the wing panels hanging below the aircraft than it was when tested in hover with

wing panels in a normal planer position. This increased controllability was attributed to the reduced moment of inertia about the aircraft's roll axis, and also due to the reduced aerodynamic damping about the roll axis with the wing panels freely rotating about their hinge. Another key consideration proved with this RC scale aircraft is that a landing procedure could be developed for first having the wingtips touch the ground and then using wheels at the wingtips to drive the wing panels outward as the the vehicle safely and controllably completed its landing. In summary, the entire wing deployment and recovery mechanism and operational procedure was proven to be feasible at an RC scale.

The second key feature proven to be feasible was the pitch axis suspended cargo pod. The RC scale helicopter was able to carry a high density (lead) 40% gross weight load without affecting longitudinal stability and control in hover and in forward flight as reported by the RC pilot. This qualitative observation matches the predicted behavior, and in the future can be verified through instrumentation and telemetry. Furthermore, when the weight was replaced by a prototypical cargo pod with stabilizer, elevator, and rudder, the entire flight profile from take-off, hover, forward flight, and landing proved to be controllable, repeatable, and feasible. Active elevator control provided for cargo pod pitch trim in hover and in forward flight, and active rudder control provided for coordinated turns in forward flight. During flight tests, the cargo pod appeared to be flying in tight coordinated formation flight with the helicopter. In summary, the design, fabrication, and operation of a pitch axis suspended cargo pod was proven to be feasible at an RC scale.

The third key feature proven feasible was the tilting centerline rotor. Control laws were developed and tested for tilting the centerline helicopter rotor shaft through 65 degrees of pitch travel while the fixed wing portion of the aircraft remained in straight and level flight. The rotor roll and yaw control inputs were mixed to correspond to rotor shaft angle for coordinated rotary and fixed wing control throughout conversion towards airplane mode and conversion back to helicopter mode. This work reduces the risk to the MTR-FD which has a centerline coaxial rotor and is expected to be flown though full conversion later this year. Furthermore, these tests provided for pilot familiarization so that operation of the MTR-FD will be similar to this flight experience.

Validation of MTR-SD design

The motivation for initiating the MTR Scaled Demonstrator (MTR-SD) project was to show that the scalable MTR concept could be implemented in a point preliminary design. In 2005, BTC organized an MTR-SD design team that included the University of Maryland

Rotorcraft Center for aerodynamic analysis and design, Eagle Aviation Technologies Incorporated for engineering design, and Army Research Labs Vehicle Technology Directorate for engineering analysis. The MTR-SD design was completed and reported in 2006 [2, 3].

Under the current AATD task order, BTC hired a separate team of aerospace engineering authorities to validate the MTR-SD design. Bell Helicopter Textron Incorporated (BHTI) applied their advanced concept preliminary design tools to perform a limited assessment of the MTR-SD vehicle, and Dr. Dimitri Mavriplis of Scientific Simulations applied his validated CFD analytical tools to assessing MTR-SD drag. Essentially, these two independent organizations checked the work of the original design team. The details of these independent assessments were reported above, and a discussion of their results follows.

Weight: BHTI found that the MTR-SD weight as was accurate to within 2% of gross weight (215 lbs / 9400 lbs). The weight budget for wing, rotor group, landing gear, propulsion group, drive system group, and load and handling group was found to be adequate. The tail group provides an opportunity for significant weight reduction. The body group, nacelle group, fixed wing flight controls group, APU group, instrument/avionics group, hydraulics group, and electrical group require further design and definition to reduce risk in achieving the weight budget. The conclusion of this weight evaluation is that the MTR-SD final reported weight has a low to medium risk of being attainable. Much of the weight risk lies in the underdeveloped or under defined areas and does not necessarily indicate a flawed weight estimate or design approach.

Drag: BHTI found through 1st order drag estimation techniques that the MTR-SD parasite drag was accurate to within 5% in aggregate for the following structures: wing panels, alighting gear, vertical and horizontal tail, struts, fuselage fairings (aka cargo pod fairings), and fuselage tail (aka cargo pod tail). Furthermore, the MTR-SD final report estimate for interference drag was comparable to the BHTI bookkeeping of protuberances, trim, and momentum drag. A striking difference was noted for the fuselage with fuel tank, and for the cargo pod. It is apparent that these structures required a more sophisticated CFD analytical treatment in order to accurately predict their drag. The CFD analysis showed that the BTC-SD final report had over predicted drag for these structures by a large margin.

Hover performance: As reported above, BHTI performed two independent assessments of hover power requirements which produced identical results within 2 % accuracy, and these results matched the MTR-SD final report plot of hover power requirements. The twin Rolls

Royce T-800 turboshaft engine power available totalling 2552 HP was found to far exceed the uninstalled hover power required of 1727 HP.

Propulsive efficiency: As reported above, BHTI performed two independent assessments of propulsive efficiency which produced identical results within 2 % accuracy. BHTI found that at cruise condition the MTR-SD rotor blade system as designed would have a propulsive efficiency of between 67% and 76% when operated in the range of 100% hover RPM to as low as 84% hover RPM. These propulsive efficiencies compare favorably to the MTR-SD final report value of 71% propulsive efficiency. Furthermore, BHTI has indicated that propulsive efficiency may be improved to as high as 83% by applying BHTI proprietary proprotor blade design techniques.

Flight dynamics: This very broad discipline encompasses the dynamic behavior of the rotor system in isolation, dynamic behavior of the full air vehicle excluding the suspended cargo pod, and dynamic behavior of the complete system including the suspended cargo pod. The MTR-SD final report included detailed rotor design and flight dynamics analysis data which BHTI independently validated using an in-house developed comprehensive rotorcraft code, COPTER. BHTI also used COPTER to confirm the limited air vehicle longitudinal dynamic data of the MTR-SD final report, and extended this analysis to include six degree of freedom mass, stiffness, and damping matrices for hover, conversion airspeed, and cruise. These matrices will be useful in future dynamic analyses of the MTR-SD.

Cruise performance: While BHTI did not have the benefit of using the CFD drag assessment data in their performance analysis, their conclusion from their less sophisticated 1st order assessment was that the range and speed capability of the MTR-SD concept, when compared to existing helicopter concepts (i.e, classic, edgewise rotorcraft whose speeds are generally limited to 120-130 ktas and whose L/D's are know to be on the range of 3-4), are significant (almost twice as fast, twice as far.) When the more accurate CFD data is incorporated into the BHTI cruise performance analysis, the predicted range exceeds the 782 nm reported in the MTR-SD final report.

Validation of MTR mission studies

Mission performance studies of the MTR air vehicle architecture performed in 2004 and 2005 [17, 18, 19] concluded that the MTR when compared to single main rotor helicopters and coaxial helicopters for long range missions of up to 1000 nm offered double the cruise speed at ½ the size, 1/3 the structural weight, and 1/3 the fuel burn. The two fundamental assumptions of these

studies were that MTR propulsive efficiency was at least 70%, and the airframe L/D was 10, for an L/D effective of 7.0. The results of the independent assessment validates these assumptions.

Conclusions

Work is underway to build and flight test key features of the Mono Tiltrotor (MTR) air vehicle architecture, integrate these features into an MTR Functional Demonstrator (MTR-FD), and also hire 3rd party engineering authorities to perform independent assessments of the MTR Scaled Demonstrator (MTR-SD). The conclusions to be drawn from the work completed to-date are as follows:

1. Aerodynamic wing deployment, wing hinge locking and unlocking, wing recovery, and landing are feasible, controllable, and repeatable at a remote control (RC) scale.
2. A pitch axis suspended cargo pod with stabilizer, elevator, and rudder is feasible at an RC scale.
3. A centerline rotor can be tilted between a helicopter mode of flight and an airplane mode of flight at an RC scale. Furthermore, control laws for steady and level flight during centerline rotor conversion have been developed and demonstrated.
4. A 50 pound gross weight MTR Functional Demonstrator (MTR-FD) designed to incorporate the folding wings, pitch axis suspended load, and a tilting coaxial rotor has been built and hover tested with the wings in a fully deployed configuration.
5. Authoritative independent assessments of the 9,400 pound gross weight MTR Scaled Demonstrator (MTR-SD) have validated the design weight, drag, hover performance, propulsive efficiency, longitudinal stability, rotor dynamics, and cruise performance. Furthermore, these assessments generated six degree of freedom stability matrices suitable for detailed flight dynamic assessment of handling qualities.
6. The authoritative independent assessments of the MTR-SD provide validation of the underlying assumptions of earlier MTR concept studies.

Acknowledgments

This work has been supported by the U.S. Army Research, Development, and Engineering Command, Aviation Applied Technology Directorate (AATD), under Contract No. W911W6-05-D-0004. The author was honored to work with the aerospace researchers at Georgia Tech, the advanced design engineers at Bell Helicopter, and Scientific Simulations in developing the information contained in this report.

References

1. "Mono Tiltrotor (MTR) Concept Evaluation", U.S. Army Contract No. W911W6-05-D-0004, 2005.
2. Baldwin, G. D., *Mono Tiltrotor (MTR) Concept Evaluation*, U. S. Army Contract Number: W911W6-04-D-0004-0001, RDECOM TR 06-D-40, DTIC Accession Number ADB324612, 2006.
3. Baldwin, G. D., "Preliminary Design Studies of a Mono Tiltrotor (MTR) with Demonstrations of Aerodynamic Wing Deployment", AHS International Specialists Meeting, Chandler, Arizona, January 23-25, 2007.
http://www.baldwintechology.com/MTR_AHS_Jan07.pdf
4. Preator, R., Leishman, J. G., Baldwin, G. D., "Conceptual Design Studies of a Mono Tiltrotor Architecture", Proceedings of the 60th Annual National Forum of the American Helicopter Society, Baltimore, MD, June 7-10, 2004.
http://www.baldwintechology.com/MTR_AHS04.pdf
5. Leishman, J. G., Preator, R., Baldwin, G. D., *Conceptual Design Studies of a Mono Tiltrotor (MTR) Architecture*, U.S. Navy Contract Number: N00014-03-C-0531, 2004.
http://www.baldwintechology.com/FY04_MTR_Conceptual_Design_Report.pdf
6. Baldwin, G. D., "Utility of a Mono Tiltrotor (MTR) Scaled Demonstrator", Proceedings of the 63rd Annual National Forum of the American Helicopter Society, Virginia Beach, VA, May 1-3, 2007.
http://www.baldwintechology.com/MTR_AHS_07_Baldwin.pdf
7. *Assessment of the Mono Tiltrotor Scaled Demonstrator*, Contract No: BTC001, Bell Helicopter Textron Incorporated, January 23, 2008.

8. Mavriplis, D., *Computational Drag Study for the Mono Tiltrotor Scaled Demonstrator (MTR-SD)*, Scientific Simulations, Inc, March 2008.

9. <http://www.baldwintechnology.com/video/btcSummer2007.mov> , accessed March 2008.

10. http://www.cad-modelltechnik-jung.de/projekte/kamov_modell_trainer.htm , accessed March 2008.

11. <http://www.jetcat.de/jetcatturbinen/helikopterturbinen.htm> , accessed March 2008.

12. <http://www.centuryheli.com/products/helikits/cn106xRAVENccpm/index.htm?currentid=46> , accessed March 2008.

13. <http://www.centuryheli.com/products/productdetail.htm?currentid=472&prtnm=CN1103> , accessed March 2008.

14. <http://aaac.larc.nasa.gov/tsab/cfdlarc/aiaa-dpw/> , accessed March 2008.

15. Mavriplis, D. J., “Results from the Third Drag Prediction Workshop using the NSU3D Unstructured Mesh Solver”, AIAA Paper 2007-0256, January 2007.

16. Yen, J. G., Corrigan, J. J., Schillings, J. J. and Hsieh, P. Y., “Comprehensive Analysis Methodology at Bell Helicopter”, AHS Aeromechanics Specialists Conference, San Francisco, CA Jan. 1994.

17. Leishman, J. G., Preator, R., Baldwin, G. D., *Conceptual Design Studies of a Mono Tiltrotor (MTR) Architecture*, U. S. Navy Contract Number: N00014-03-C-0531, 2004.

http://www.baldwintechnology.com/FY04_MTR_Conceptual_Design_Report.pdf

18. Preator, R., Leishman, J. G., and Baldwin, G. D., “Conceptual Design Studies of a Mono Tiltrotor (MTR) Architecture,” Proceedings of the 60th Annual Forum of the American Helicopter Society International, Baltimore, MD, June 7–11, 2004.

http://www.baldwintechnology.com/MTR_AHS04.pdf

19. Preator, R., Leishman, J. G., and Baldwin, G. D., “Performance and Trade Studies of Mono Tiltrotor Design,” Proceedings of the 61st Annual Forum of the American Helicopter Society International, Grapevine, TX, June 1–3, 2005.

http://www.baldwintechnology.com/MTR_AHS05.pdf